Moroccan Journal of Chemistry
ISSN: 2351-812X
http://revues.imist.ma/?journal=morjchem&page=login
El-Bagoury & al. / Mor. J. Chem. 5 N°3 (2017) 438-445

Microstructure and corrosion behaviour of NiTiCo shape memory alloys under various aging conditions

Nader El-Bagoury [(a,b)] **, *K.F. Khaled*** [(a,c)*]

[(a)]*Chemistry Department, Faculty of Science, TAIF University, P.O. Box 888, El-Haweyah, El-Taif, Saudi Arabia.*
[(b)]*Casting Technology Lab., Manufacturing Technology Dept., Cmrdi, Central Metallurgical Research and Development Institute, P.O. Box 87, Helwan, Cairo, Egypt.*
[(c)]*Electrochemistry Research Lab., Chemistry Department, Faculty of Education, Ain Shams University, Roxy, Cairo, Egypt.*

** Corresponding author:*
khaledrice2003@yahoo.com
Received 14 Jan 2017,
Revised 25 May 2017,
Accepted 11 Jun 2016

Abstract

In this study the microstructure evolution and corrosion resistance of NiTiCo and Co-free NiTi shape memory alloys (smart alloys) were investigated under various aging conditions. Cobalt NiTi alloy contains 4 at% in addition to 52 at% Nickel and 44 at% Titanium, while in Co- free alloy Titanium content increased to 48 at%. Optical and scanning electron microscopes were used to investigate the microstructure evolution of NiTi alloys. Potentiodynamic polarization measurements were used to study the corrosion behavior of the tested alloys in 1.0 M HCl solution at 25 °C. The results show that martensite phase, B19', is predominant phase in the aged microstructures of the investigated alloys. Moreover, there is an intermetallic compound phase, Ti_2Ni, that precipitated in various densities and sizes in microstructures depending on the aging heat treatment conditions. Polarization measurements show that the corrosion rate of the NiTi alloys increases as the aging temperature increase. Also, potentiodynamic polarization shows that the addition of 4% of cobalt as alloying element decreases the corrosion rate.

Keywords: *Aging heat treatment, NiTi SMA, structure, corrosion resistance, Potentiodynamic Polarization.*

1. Introduction

In the past decades NiTi shape memory alloys (SMAs) have received considerable interest [1–4] because they combine excellent functional properties (one way effect, superelasiticity) with very good mechanical strength and ductility. Moreover they exhibit good corrosion resistance (which is important in medical applications) and high specific electric resistance (which allows the materials to be easily heated using an electric current). The functional properties of SMAs are due to a martensitic phase change. This occurs in simple systems between one high temperature phase (austenite) and one low temperature phase (martensite) [3, 4]. There is an interest in Ni-rich NiTi alloys because phase transition temperatures can be controlled through the Ni-content [2, 5]. The commercialization of shape memory alloys, and specifically nitinol, is a truly unique success story. The discovery of shape memory in Au–Cd and Cu–Zn occurred with little fanfare in somewhat obscure technical papers with little, if any, follow-on work. However, when the shape memory effect was rediscovered in equiatomic Ni–Ti in 1962, there was suddenly a great deal of commercial interest [6]. Fujishima et al. have been reported that appearance and disappearance of multistage martensitic transformation in Ni-rich NiTialloys depends on the atmosphere of heat treatment. They have also proposed that the atmosphere of annealing at high temperature is more important than aging atmosphere at 500 ◦C [7]. As reported in a number of studies [8–18], to improve shape memory and mechanical properties, the alloys are usually aged at an appropriate temperature that may give rise to the precipitation of second phases from the supersaturated matrix. Although the focus of a majority of these studies has been the shape memory effect, considerable amounts of data have been made available on the change of Ms temperature as a result of aging. The temperature alterations are suggested to be affected by precipitation hardening and a change of the matrix composition [8]. However, no satisfactory explanation has been offered as to how the compositional change of the matrix influences the Ms temperature. During ageing coherent metastable particles of type Ni_4Ti_3 can be observed using transmission electron microscopy (TEM) [19, 20]. Ni_4Ti_3 particles coherently precipitate in the B2 matrix. In any cases such particle/matrix systems are found to transform in two stages, first from B2 to a trigonal R-phase and then from R into B19’ martensite [21]. The change from a one-step to a two-step transformation in NiTi SMAs is understandable because both R-phase and B19’ are potential martensite candidates. This is suggested by the observation of corresponding soft phonons in inelastic neutron scattering experiments [22]. In the absence of particles, the one-step transformation of B2 to B19’ occurs. But the presence of coherent particles produces a strong resistance to large lattice variant deformations associated with the formation of B19’. The aim of this study is to investigate the effect of aging temperature on the microstructure and corrosion characteristics of the NiTi shape memory alloys. Moreover, the role played with the addition of 4% cobalt to the NiTi alloy on the corrosion resistance of these alloys will be investigated.

2. Experimental work

Polycrystalline Co-free NiTi and NiTiCo (4 at% Co) shape memory alloys were manufactured by melting pure elements (more than 99.99% purity) in an induction vacuum furnace. These alloys were melted four times to ensure homogeneity and cast into an investment casting ceramic mould. This mould was preheated to 1000°C before pouring process of the molten metal. Specimens from these alloys were solutionized at 1000°C for 24 h followed by quenching in iced water. The aging heat treatment processes were carried out at various temperatures ranging from 300 to 600°C for 3 h then iced water quenching. Optical emission apparatus, ARL3560OES as well as Ni base software were used to determine the chemical composition of the heat treated alloys. Characterization for microstructure studies including morphology and volume fraction of different phases was carried out by both Zeiss light optical microscope fitted with Hitachi digital camera and JOEL JSM-5410 Scanning Electron Microscope (SEM). The specimens for microstructure examination were ground and polished according to ASTM standard E3 and E768, then etched with solution of HNO_3,

HF and H_2O in a ratio of 4: 1: 5 respectively, to reveal the Ti_2Ni precipitates. To examine the martensite phase, another etching solution of HNO_3/HF/CH_3COOH in a ratio of 4: 4: 2 was used. The microanalysis for different phases in the microstructure was performed using EDS in JEOL JSM5410. Electrochemical measurements were carried out in a conventional electrochemical cell containing three compartments for working, a platinum foil (1.0 cm^2) counter and reference electrodes. A Luggin-Haber capillary was also included in the design. The tip of the Luggin capillary is made very close to the surface of the working electrode to minimize IR drop. The reference electrode was a silver silver chloride electrode used directly in contact with the working solution. The experiments were conducted in 150 cm^3 volume cell at 25 ^oC ±2 using a temperature control water bath. Polarization measurements were carried out starting from a cathodic potential of -2.0 V to an anodic potential of +2.0 V vs Ag/AgCl at a sweep rate of 5 mV s^{-1}. The linear Tafel segments of the cathodic and anodic curves were extrapolated to corrosion potential to obtain the corrosion current densities (i_{corr}). All Electrochemical experiments were carried out using Gamry 3000 Potentiostat/Galvanostat/Zra analyzer, DC105 Corrosion software.

3. Results and Discussions

3.1 Microstructure Evolution

The structures of the studied cobalt free NiTi and NiTiCo (4 at% cobalt) shape memory alloys under various aging conditions are shown in Fig. 1. The microstructure of the investigated alloys consists of martensite phase, B19', in addition to precipitation of Ti_2Ni phase. The density and the size of Ti_2Ni precipitate as well as the thickness of the martensite phase lath in the microstructure are influenced by the aging heat treatment conditions. Both cobalt free NiTi and NiTiCo alloys, after casting process, were initially solutionized at 1000 °C for 24h followed by iced water quenching. After that these alloys were heat treated by aging at various temperatures of 300, 400, 500 and 600 °C for 3h then quenched in iced water.

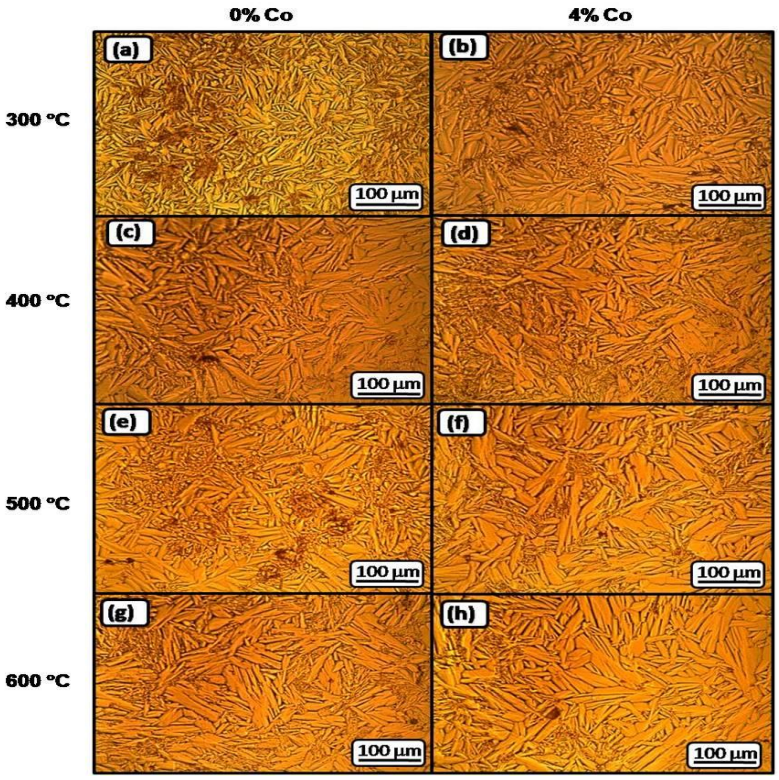

Figure 1. Martensitic structures in aged Co-free NiTi and NiTiCo alloys at 250 °C (a) and (b), at 350 °C (c) and (d), at 450 °C (e) and (f) and at 550 °C (g) and (h), respectively.

The matrix in microstructures of both alloys is fully martensitic where the parent phase, austenite (B2), completely transformed to martensite. This is evidence that the martensitic phase transformation temperatures are higher than room temperature for all aged specimens with different aging temperatures. Aging heat treatment elevates the martensitic phase transformation [23]. Moreover, as the aging temperature increase the martensitic phase transformation temperature increase [24, 25]. It is clearly shown in Fig. 1 where as the aging temperature increases the lath thickness of the martensite phase increases in case of both Co-free NiTi and NiTiCo specimens. Compared to Co-free NiTi specimens, the corresponding NiTiCo specimens have thicker lath of martensite phase.

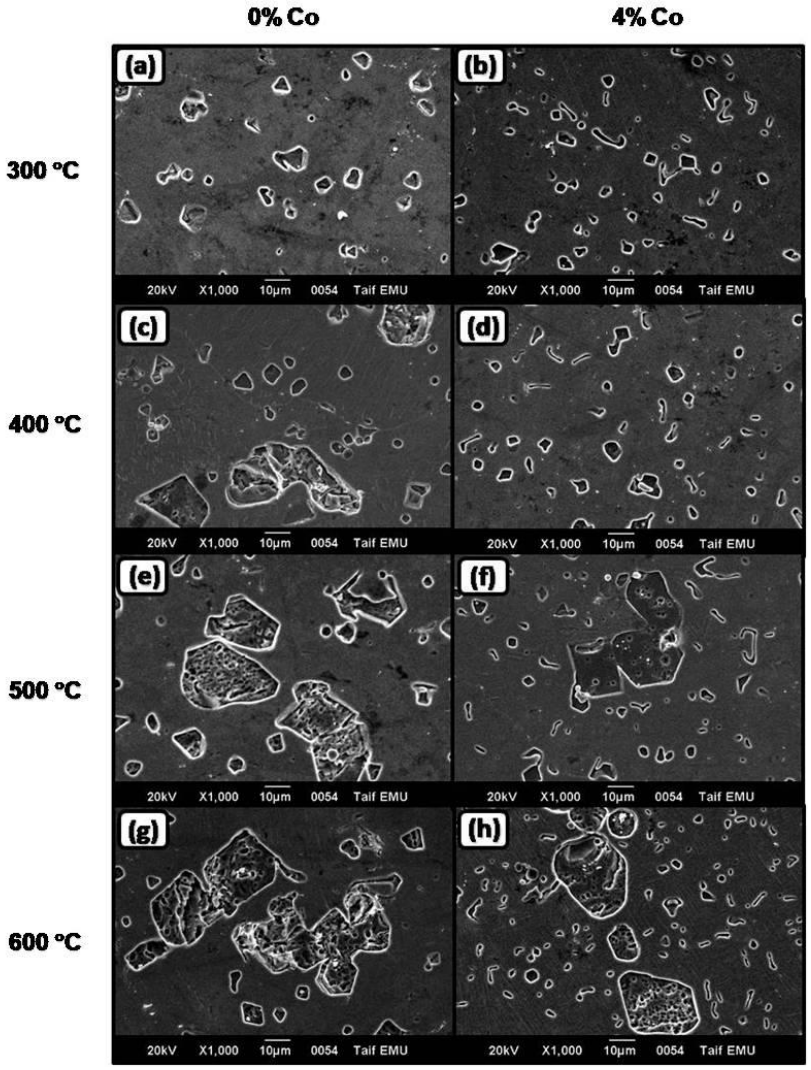

Figure 2. Precipitation of Ti_2Ni phase in aged microstructures of Co-free NiTi and NiTiCo alloys at 250 °C (a) and (b), at 350 °C (c) and (d), at 450 °C (e) and (f) and at 550 °C (g) and (h), respectively.

Additionally, aging temperature as well as cobalt content in NiTi shape memory alloy affects the density and size of Ti_2Ni precipitates in microstructures. As illustrated in Fig. 2, the precipitated Ti_2Ni phase get coarser in size by elevating aging temperature from 300 to 600 °C in both studied alloys. Meanwhile, it is obviously noted that size of Ti_2Ni precipitates in Co-free NiTi specimens (Fig. 2 a, c, e and g) is larger than in the counterpart specimens of NiTiCo alloy (Fig. 2 b, d, f and h). In addition to the size of Ti_2Ni precipitates, its density increases as the aging temperature increase in both alloys. However, the density of Ti_2Ni phase in the NiTiCo specimens is higher than in the corresponding Co-free NiTi specimens.

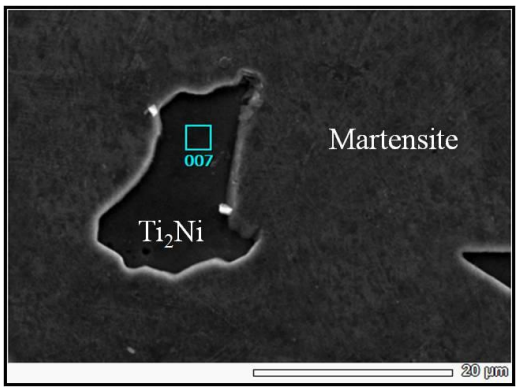

Figure 3. Ti_2Ni precipitates in microstructure of Co-free NiTi specimen aged at 400 °C.

Table 1. EDS chemical analysis of Ti2Ni in Co-free NiTi and NiTiCo alloys.

Elements / Phase	Ti	Ni	Co
Ti_2Ni (0 at% Co)	65.97	34.03	0.00
Ti_2Ni (4 at% Co)	62.26	34.87	2.87

Figure 3 shows one of the Ti_2Ni precipitates, surrounded by martensite matrix, which found in the microstructure of Co-free NiTi specimen aged at 400 °C. The micro-chemical analysis of Ti_2Ni precipitated in NiTi and in NiTiCo alloys are listed in Table 1. Ti_2Ni precipitated in NiTiCo specimens has a definite content of Co that presented at the expense of Ti percentage.

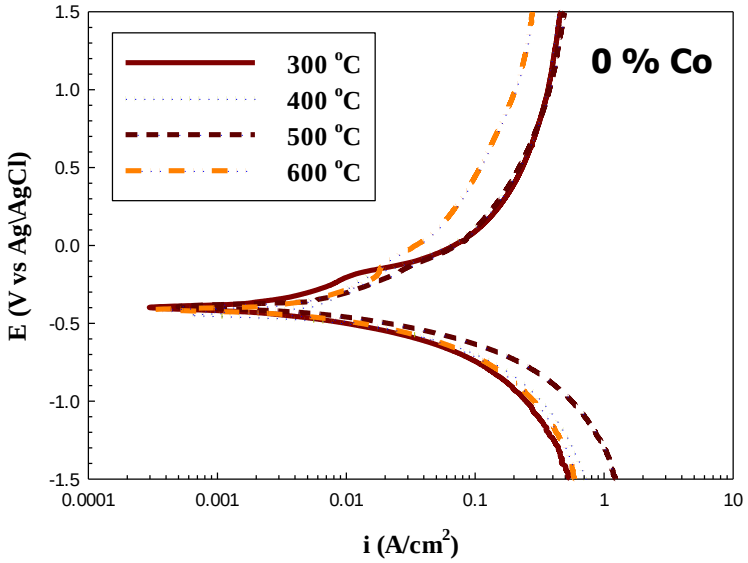

Figure 4. Potentiodynamic polarization curves recorded for Co-Free NiTi alloy, as a function of aging temperature, in 1.0 M HCl solution at a scan rate of 5 mV s^{-1} at 25 °C.

3.2.Corrosion Behaviour

Figures 4-5 present, respectively, the cathodic and anodic polarization curves recorded for NiTi and NiTiCo alloys in aerated stagnant 1.0 M HCl solutions at a scan rate of 5 mV s^{-1} at 25 °C. It is obvious, in all cases, that both the anodic and cathodic branches of the polarization curves display Tafel behaviour within a definite potential range. The values

of the corrosion current density (i_{corr}), and the other electrochemical parameters, for the studied alloys corrosion reaction in 1.0 M HCl were determined. therefore by extrapolation of the cathodic and anodic Tafel lines to the corrosion potential (E_{corr}).

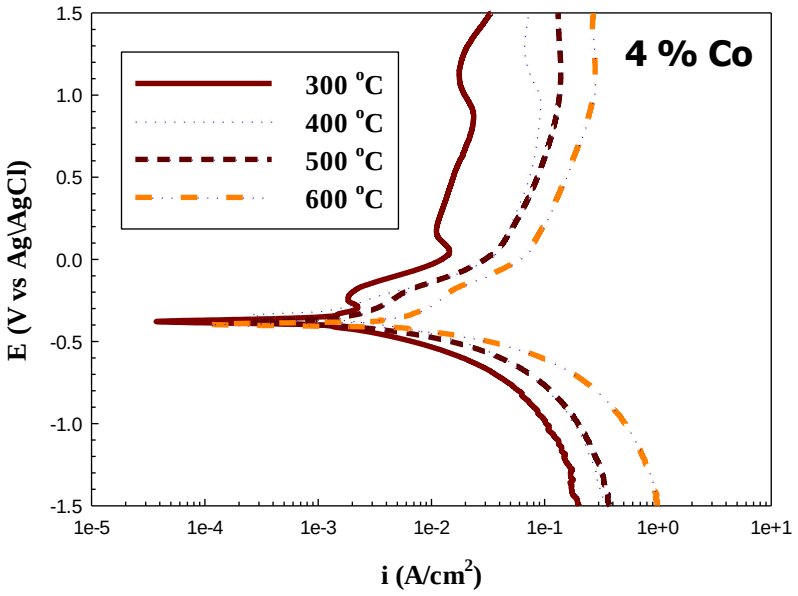

Figure 5. Potentiodynamic polarization curves recorded for NiTi alloy containing 4% Co, as a function of aging temperature, in 1.0 M HCl solution at a scan rate of 5 mV s^{-1} at 25 °C.

Table 2 collects these parameters as a function of aging temperature of the alloys. It follows from Fig. 4 that the cathodic reaction is markedly affected by the aging temperature, while the anodic one is slightly shifted toward higher current densities. From Table 2, there are no definite shift in the corrosion potential and the marked increase of the cathodic current density upon increasing the aging temperature of the alloys.

Table 2. Electrochemical kinetic parameters and rates of corrosion (C.R) associated with Tafel polarization measurements recorded for alloy in 1.0 M HCl solutions.

Alloy	Temp	βa / V dec^{-1}	-βc / V dec^{-1}	-E_{corr} / V(SCE)	(i_{corr}) / mA cm^{-2}	Corrosion rate (C.R) / mpy
0 % Co	300	0.306	0.2	0.401	3.00	1372
	400	0.484	0.196	0.447	5.98	2731
	500	0.373	0.183	0.398	6.14	2.788
	600	0.640	0.229	0.415	7.53	3443
4% Co	300	0.916	0.247	0.381	3.30	1005
	400	0.491	0.275	0.338	4.43	1927
	500	0.647	0.268	0.384	5.84	2211
	600	0.440	0.163	0.395	6.55	2995

Figure 6 shows the effect of addition of 4% cobalt as an alloying element in the enhancement of the corrosion resistance of the NiTiCo alloys. Addition of 4% cobalt enhances the corrosion resistance of NiTiCo alloys at all aging temperatures (Table 2, Figure 6).

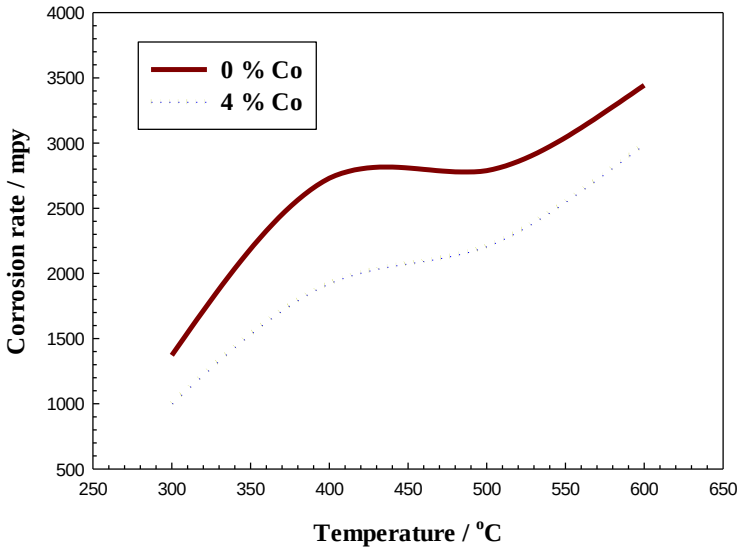

Figure 6. Corrosion resistance vs aging temperature in absence and presence of Co in NiTi alloy.

It can be concluded that the elevating aging temperature leads to increase the density and the size of Ti_2Ni precipitates in the microstructure of the investigated both co-free NiTi and NiTiCo alloys. The increase of density and size of Ti_2Ni phase taken place at the expense of Ni and Ti content in the matrix, martensite phase. The depletion of Ni and Ti percentages in the martensite phase lowers the corrosion resistance of the matrix phase. At lower aging temperatures, the martensite phase has higher Ni and Ti contents, which in turn helps the formation of the oxide layer passivation of Ni and Ti oxides. This advantage is missed in the specimens that aged at higher temperatures, at 500 and 600 °C, decreasing the corrosion resistance of these aged specimens. The presence of Co alloying element in NiTiCo alloy compensate the depletion of Ti content in martensite phase and enhances the corrosion resistance of Co alloy compared to Co-free NiTi alloy.

4. Conclusions

- The structure of the investigated NiTi and NiTiCo specimens consists of martensite phase, B19', in addition to Ti_2Ni precipitates in various densities and sizes under studied aging conditions.
- Martensite phase lath is coarser in the case of NiTiCo alloy than in Co-free NiTi alloy. In both alloys, the thickness of martensite lath increased by increasing aging temperature.
- NiTiCo alloy have lower densities and smaller sizes for the inter-metallic compound Ti_2Ni precipitates in comparison with counterpart free cobalt NiTi alloy. Elevating aging temperature increases the density and size of Ti_2Ni phase in the microstructure of both alloys.
- Compared to the Co-free NiTi alloy, the NiTiCo alloy exhibited higher corrosion resistance.
- Potentiodynamic polarization measurements showed that the corrosion resistance of the studied alloys decreases with the increase in the aging temperature.

Acknowledgements

The authors acknowledge the financial aid received from Taif University, Saudia Arabia (Project No. 1/437/4758).

References

[1] E. Hornbogen In: Bunk WGJ, editor. Advanced structural and functional materials. Heidelberg: Springer-Verlag; 1991. p. 133–63.

[2] T. Saburi In: K. Otsuka, C.M. Wayman, editors. Shape memory materials. Cambridge: Cambridge University Press; 1998. p. 49–96.

[3] Y. X. Tong, P. C. Jiang, F. Chen, B. Tian, L. Li, Y. F. Zheng, D. V. Gunderov, R. Z. Valiev, *Intermetallics* 49 (2014) 81-86.

[4] B. Karbakhsh Ravari, M. Nishida, *Philos. Mag.*, 93 (2013) 2279-2296.

[5] X. Wang, B. Verlinden, J. Van Humbeeck, *Mater. Today Proc.*, 2 (2015) 565-568.

[6] D. T. Zhang, B. Guo, Y. X. Tong, B. Tian, L. Li, Y. F. Zheng, D. Gunderov, R. Valiev, *Trans. Nonferr. Met. Soc. China* 26 (2016) 448-455.

[7] K. Fujishima, M. Nishida, Y. Morizono, K. Yamaguchi, K. Ishiuchi, T. Yamamuro, *Materials Science and Engineering A*, 438–440 (2006) 489–494.

[8] K. Otsuka, X. Ren, *Prog Mater Sci*, 50 (2005) 511–678.

[9] H. C. Lin, C. H. Yang, M. C. Lin, C. S. Lin, K. M. Lin, L. S. Chang, *J Alloys Compd*, 449 (2008) 119–124.

[10] Y. X. Tong, Ph.D. thesis, Nanyang Technological University, Singapore; 2008.

[11] X. L. Meng, Y. F. Zheng, Z. Wang, L. C. Zhao, *Scr Mater*, 42 (2000) 341–348.

[12] L. Patriarca a , Y. Wu , Huseyin Sehitoglu, Y.I. Chumlyakov, *Scripta Materialia*, 115 (2016) 133–136.

[13] J. Khalil-Allafi, G. Eggeler, W. W. Schmahl D. Sheptyakov, *Mater Sci Eng A*, 438–440 (2006) 593–596.

[14] M. Peltonen, T. Lindroos, M. Kallio, *J Alloys Compd*, 460 (2008) 237–245.

[15] X. L. Meng, W. Cai, Y. D. Fu, Q. F. Li, J. X. Zhang, L.C. Zhao, *Intermetallics*, 16 (2008) 698–705.

[16] T. Sawaguchi, M. Sato, A. Ishida, *Mater Sci Eng A*, 332 (2002) 47–55.

[17] Q. Tian, J. Wu, *Intermetallics*, 10 (2002) 675–682.

[18] Y.X. Tong a , K.P. Hu a , F. Chen , B. Tian, L. Li , Y.F. Zheng, *Intermetallics*, 85 (2017) 163-169.

[19] A. Amir, S. Atiq, W. Ahmad, A. Saleem, and H. Haseebah, *A. Physical and Computational Sciences*, 54 (1) (2017) 89–93.

[20] T. Tadaki, Y. Nakata, K. Shimizu, K. Otsuka, *Trans JIM*, 27 (1986) 731.

[21] T. Saburi In: K. Otsuka, C.M. Wayman, editors. Shape memory materials. Cambridge: Cambridge University Press; 49 (1998) 96.

[22] X. Ren, N. Miura, K. Taniwaki, K. Otsuka, T. Suzuki, K. Tanaka, Y.I.. Chumlyakov, M. Asai, *Mater Sci Eng*, A273–275 (1999) 190-194.

[23] N. El-Bagoury, *Materials at High Temperatures*, 32 (4) (2015) 390-398.

[24] N. El-Bagoury, *Materials Science and Technology*, 30 (14) (2014) 1795- 1800.

[25] Nader El-Bagoury, *Met. Mater. Int.*, 22 (3) (2016) 468-473.